

# Fluorescence Turn-On Chemosensor for Highly Selective and Sensitive Detection and Bioimaging of Al<sup>3+</sup> in Living Cells Based on Ion-Induced Aggregation

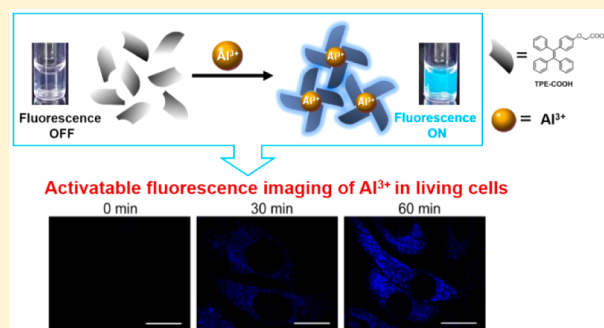
Shilang Gui,<sup>†</sup> Yanyan Huang,<sup>‡</sup> Fang Hu,<sup>‡</sup> Yulong Jin,<sup>‡</sup> Guanxin Zhang,<sup>‡</sup> Liushui Yan,<sup>\*,†</sup> Deqing Zhang,<sup>\*,‡</sup> and Rui Zhao<sup>\*,‡</sup>

<sup>†</sup>School of Environment and Chemical Engineering, Nanchang Hangkong University, Nanchang 330063, China

<sup>‡</sup>Beijing National Laboratory for Molecular Sciences, CAS Key Laboratories of Analytical Chemistry for Living Biosystems and Organic Solids, Institute of Chemistry, Chinese Academy of Sciences, Beijing 100190, China

## Supporting Information

**ABSTRACT:** Herein, a new fluorescence turn-on chemosensor 2-(4-(1,2,2-triphenylvinyl)phenoxy)acetic acid (TPE-COOH) specific for Al<sup>3+</sup> was presented by combining the aggregation-induced-emission (AIE) effect of tertaphenylethylene and the complexation capability of carboxyl. The introduction of carboxylic group provides the probe with good water-solubility which is important for analyzing biological samples. The recognition toward Al<sup>3+</sup> induced the molecular aggregation and activated the blue fluorescence of the TPE core. The high selectivity of the probe was demonstrated by discriminating Al<sup>3+</sup> over a variety of metal ions in a complex mixture. A detection limit down to 21.6 nM was determined for Al<sup>3+</sup> quantitation. Furthermore, benefiting from its good water solubility and biocompatibility, imaging detection and real-time monitoring of Al<sup>3+</sup> in living HeLa cells were successfully achieved. The AIE effect of the probe enables high signal-to-noise ratio for bioimaging even without multiple washing steps. These superiorities make this probe a great potential for the functional study and analysis of Al<sup>3+</sup> in complex biosystems.



Aluminum, the most abundant metal of the Earth's crust, plays an important role in alimentary production, pharmaceutical drugs, as well as the aerospace industry.<sup>1</sup> Nowadays, because of acidic rain and human activities in the environment, increasing exposure to free aluminum ions (Al<sup>3+</sup>) poses a severe threat to biospheres and human health.<sup>2,3</sup> Excessive intake of Al<sup>3+</sup> has been demonstrated to cause a wide range of diseases by accumulating in different organs of living organisms.<sup>4</sup> The deleterious effect of Al<sup>3+</sup> toward the central nervous system further makes the population at high risk for various neurodegenerative diseases.<sup>5,6</sup> In this regard, detection of Al<sup>3+</sup> in living biosystems is of great importance, not only for monitoring aluminum contamination but also for understanding its biological functions.

Fluorescent chemosensors are receiving considerable attention owing to their rapidity, convenience, and sensitivity for analysis.<sup>7–10</sup> Several molecular probes based on fluorescence off-on and/or ratiometric strategy have been reported.<sup>11–14</sup> Nevertheless, effective design of an Al<sup>3+</sup>-specific fluorescence sensor is still challenging, arising from relative weak coordination and strong hydration abilities of Al<sup>3+</sup>.<sup>4</sup> The detection of Al<sup>3+</sup> can be easily interfered with by the matrix, leading to limited selectivity and sensitivity.<sup>15–17</sup> Moreover, poor water-solubility is another obstacle of many existing

fluorescence probes,<sup>11,18</sup> which severely prevents their further application in environmental and biological systems.

Recently, fluorogens with an aggregation-induced emission (AIE) effect have attracted remarkable research attention.<sup>19–21</sup> Their unique fluorescence behavior makes them nonemissive or weakly fluorescent in free solution but become highly emissive upon aggregation.<sup>22,23</sup> Benefiting from such activatable fluorescence signal, chemo- and biosensors have been developed for analyzing various species including ions,<sup>24,25</sup> DNA,<sup>26</sup> proteins,<sup>27</sup> and cancer cells.<sup>28,29</sup> As Al<sup>3+</sup> is concerned, Dong and colleagues designed a benzoate-based AIE probe.<sup>30</sup> Tang and co-workers used pyridinyl-functionalized tertaphenylethylene for the sensing of trivalent ions including Cr<sup>3+</sup>, Fe<sup>3+</sup>, and Al<sup>3+</sup>.<sup>31</sup> However, these reported AIE fluorogens usually work in pure organic or organic-aqueous solvents (with high content of organic reagents), resulting in the insufficient biocompatibility.<sup>32</sup> Hence, novel AIE probes with high selectivity and sensitivity is highly desirable for Al<sup>3+</sup> quantitation and bioimaging.

**Received:** November 4, 2014

**Accepted:** January 20, 2015

Herein, a new AIE fluorescence probe 2-(4-(1,2,2-triphenylvinyl)phenoxy)acetic acid (TPE-COOH) was presented with the above desired properties for  $\text{Al}^{3+}$  analysis. The introduction of a carboxyl group into tertaphenylethylene not only significantly enhanced the water-solubility, more importantly, it also enabled the specific complexation of  $\text{Al}^{3+}$ . The mechanism investigation demonstrated that the particular molecular structure of TPE-COOH gives rise to the high selectivity toward  $\text{Al}^{3+}$ . Taking advantage of the AIE effect, fluorescence turn-on bioimaging of  $\text{Al}^{3+}$  in living cells confirms the great potential of the probe in analyzing living biosystems.

## EXPERIMENTAL SECTION

**Synthesis of TPE-COOH.** 4-(1,2,2-Triphenylvinyl)phenol (compound 1) was prepared according to the reported procedures,<sup>33</sup> which was allowed to react with methyl bromoacetate in the present of  $\text{K}_2\text{CO}_3$  to obtain methyl 2-(4-(1,2,2-triphenylvinyl)phenoxy)acetate (compound 2) in 82% yield. The methanol solution (10 mL) of compound 2 (420.0 mg, 1.0 mmol) was mixed with NaOH aqueous solution (1 mL, 2.0 M) and stirred at room temperature. After 3 h, white crystal solid was precipitated in the mixture. TPE-COOH (381.8 mg, 0.94 mmol) was obtained through filtration.  $^1\text{H}$  NMR (400 MHz,  $\text{CD}_3\text{OD}$ );  $\delta$  7.05 (m, 9H), 6.98 (m, 6H), 6.88 (d,  $J = 8.8$  Hz, 2H), 6.66 (d,  $J = 8.8$  Hz, 2H), 4.43 (s, 2H).  $^{13}\text{C}$  NMR (75 MHz,  $\text{CD}_3\text{OD}$ ,  $\delta$ ): 173.0, 157.0, 144.0, 143.9, 140.6, 140.3, 136.5, 132.1, 131.0, 127.4, 127.3, 126.1, 126.0, 125.9, 113.5, 65.6. HRMS (MALDI): calcd for  $\text{C}_{28}\text{H}_{22}\text{O}_3$  [M], 406.1569; found, 406.1567.

**General Procedure for Fluorescence Measurement.** Stock solutions of various metal ions (0.25 mM) were prepared with ultrapure water, respectively. A stock solution of TPE-COOH (1 mM) was prepared with DMSO. For a typical detection, TPE-COOH solution was mixed with the stock solution of one metal ion, followed by the dilution with appropriate amounts of water or water/acetonitrile. After the incubation at room temperature for 30 min, the corresponding fluorescence spectrum was recorded; the excitation wavelength was 310 nm and the emission was collected from 350 to 600 nm.

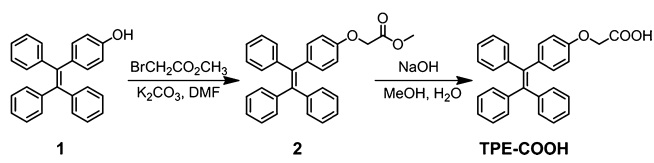
**Fluorescence Imaging of  $\text{Al}^{3+}$  in Living Cells.** The adherent HeLa cells were washed with HEPES buffer three times and first loaded with  $\text{Al}^{3+}$  (50  $\mu\text{M}$  in culture media) at 37  $^\circ\text{C}$  for 60 min. After removal of free  $\text{Al}^{3+}$  by washing the cells with HEPES buffer, TPE-COOH (20  $\mu\text{M}$  in HEPES containing 2% DMSO) was added to stain the cells for 30 min. The fluorescence images were collected directly by an Olympus FV1000-IX81 confocal-laser scanning microscope without further washing steps.

## RESULTS AND DISCUSSION

**Design and Synthesis.** Given that oxygen can provide a hard-base environment for the hard-acid  $\text{Al}^{3+}$ ,<sup>34</sup> a carboxylic group was introduced to functionalize TPE. The oxygen donor sites of the carboxyl group were expected to induce the binding of the probe toward  $\text{Al}^{3+}$ . Furthermore, the molecular aggregation effect of TPE structure was anticipated to reinforce the stability of the complex and provide activatable fluorescence for  $\text{Al}^{3+}$  sensing. The chemical structure of the target probe TPE-COOH and its synthetic process are depicted in Scheme 1. After purification, TPE-COOH was obtained with a yield of

94% and characterized by  $^1\text{H}$  NMR,  $^{13}\text{C}$  NMR, HRMS, and HPLC (Figures S-1–S-3, Supporting Information).

### Scheme 1. Chemical Structures and Synthetic Routes to TPE-COOH



**Fluorescence Turn-On Sensing of  $\text{Al}^{3+}$ .** The AIE behavior of TPE-COOH was first verified by measuring its fluorescence spectra in different mixed solvents (Supporting Information, Figure S-4). With the attempt for the fluorescence turn-on sensing of  $\text{Al}^{3+}$  in biological samples, TPE-COOH itself should be fluorescence-silent in aqueous environment and becomes strongly emissive while coexisting with  $\text{Al}^{3+}$ . By using the biological compatible DMSO as the additive, a nonemissive TPE-COOH solution was obtained even when the water content was as high as 98% (Figure 1a). Upon the addition of  $\text{Al}^{3+}$ , the expected blue fluorescence was switched on with a 52-fold enhanced fluorescence intensity at 470 nm. Such blue fluorescence can be detected by the naked-eye under UV light (Figure 1a, insert). Correspondently, DLS analysis shows that large aggregates were formed with an average diameter of 210 nm (Figure S-5, Supporting Information). Such nanoaggregates were also clearly observed by transmission electron microscopy (TEM) (Figure 1a, Figure S-6 in the Supporting Information). These results suggest that  $\text{Al}^{3+}$  ions can initiate the aggregation of TPE-COOH and result in the significant fluorescence emission.

To investigate such an  $\text{Al}^{3+}$ -induced fluorescence turn-on phenomenon, the chelation effect was first examined. The competitive binding assay was carried out by incubation of  $\text{Al}^{3+}$  and TPE-COOH with a typical chelating reagent EDTA. As shown in Figure 1a, the existence of EDTA almost completely disabled the fluorescence emission, owing to the coordination ability of the four carboxylates in EDTA toward  $\text{Al}^{3+}$ . The strong coordinative EDTA occupied the sites on  $\text{Al}^{3+}$  and thus blocked the binding of TPE-COOH to  $\text{Al}^{3+}$ . To confirm this, a structural analogue TPE-N3, which has the same tertaphenylethylene core but is substituted with an azide group, was used as a control. Without the carboxyl group, TPE-N3 cannot interact with  $\text{Al}^{3+}$  and no fluorescence change was detected after  $\text{Al}^{3+}$  treatment (Figure S-7 in the Supporting Information). This result clearly demonstrates the important role of the carboxyl group on TPE-COOH for  $\text{Al}^{3+}$  binding.

**Selectivity of the Probe toward  $\text{Al}^{3+}$ .** To study the selectivity of the probe, 15 metal ions with different valences were examined as the alternative of  $\text{Al}^{3+}$  for the incubation with TPE-COOH. As shown in Figure S-8 (Supporting Information), none of these ions can turn on the fluorescence of TPE-COOH under the same conditions, except  $\text{Pb}^{2+}$ . The fluorescence variation caused by  $\text{Pb}^{2+}$  was 57% of that induced by  $\text{Al}^{3+}$ . To eliminate the interference from  $\text{Pb}^{2+}$ , acetonitrile was chosen as the mask reagent based on its coordination ability toward heavy metal ions.<sup>35,36</sup> To acquire ideal mask efficiency, the content of acetonitrile was optimized as 5% (Figure S-9 in the Supporting Information). Under this condition, only  $\text{Al}^{3+}$  can induce distinct blue fluorescence,

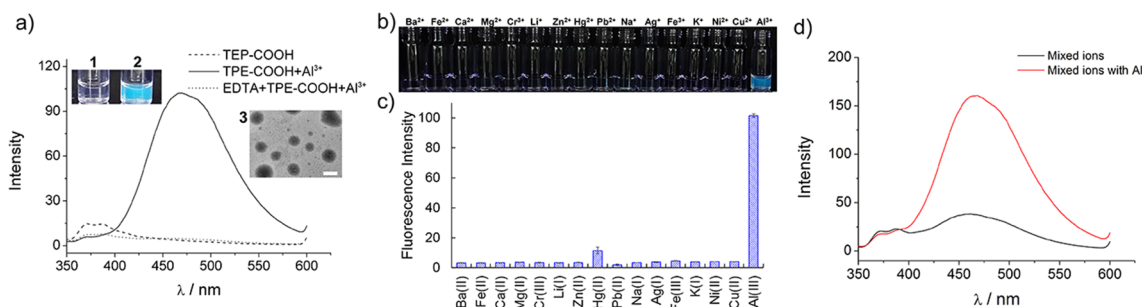


**Figure 1.** (a) Fluorescence spectra of TPE-COOH (20 μM, DMSO/H<sub>2</sub>O = 2:98) in the absence and presence of Al<sup>3+</sup> (10 μM), and fluorescence spectrum for the mixture of TPE-COOH, Al<sup>3+</sup>, and EDTA. Inset: photographs of (1) TPE-COOH, (2) TPE-COOH + Al<sup>3+</sup> solutions taken under UV light, and (3) TEM image of nanoaggregates (scale bar, 200 nm). (b) Photographs of TPE-COOH (20 μM) aqueous solutions (2% DMSO, 5% CH<sub>3</sub>CN) added with the individual metal ion under UV light; (c) fluorescence intensity of the above metal ion-added TPE-COOH solutions; (d) fluorescence spectra of TPE-COOH (20 μM) aqueous solutions (2% DMSO, 5% CH<sub>3</sub>CN) in the presence of various metal ions (Ba<sup>2+</sup>, Fe<sup>2+</sup>, Ca<sup>2+</sup>, Mg<sup>2+</sup>, Cr<sup>3+</sup>, Li<sup>+</sup>, Zn<sup>2+</sup>, Hg<sup>2+</sup>, Pb<sup>2+</sup>, Na<sup>+</sup>, Ag<sup>+</sup>, Fe<sup>3+</sup>, K<sup>+</sup>, Ni<sup>2+</sup>, and Cu<sup>2+</sup>) with and without Al<sup>3+</sup> (each 10 μM).

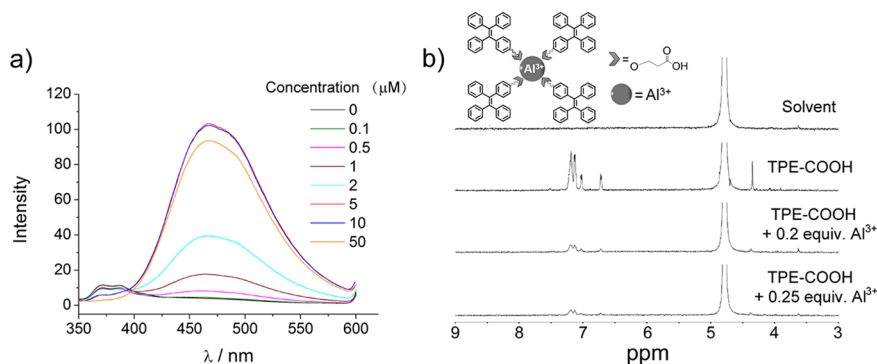


**Figure 2.** (a) Fluorescence spectra of TPE-COOH (20 μM) upon addition of different amounts of Al<sup>3+</sup>. (b) <sup>1</sup>H NMR spectra of TPE-COOH without and with AlCl<sub>3</sub>·6H<sub>2</sub>O in DMSO-d<sub>6</sub>/D<sub>2</sub>O; inset: possible binding mode between TPE-COOH and Al<sup>3+</sup>.

while TPE-COOH still remains fluorescence silence after incubating with the other metal ions (Figure 1b,c).

Furthermore, to verify the ability of the probe to discriminate Al<sup>3+</sup> in complex samples, Al<sup>3+</sup> was analyzed in the mixture of the above 15 metal ions. Without any pretreatment, the mixed ion solution containing Al<sup>3+</sup> releases significant fluorescence, while fluorescence signal from the solution only consisting of 15 control ions is negligible (Figure 1d). These results clearly indicate the high selectivity of TPE-COOH for Al<sup>3+</sup> over other species, which can facilitate the practical detection of Al<sup>3+</sup> in complex biological samples.

**Sensitive Quantitation of Al<sup>3+</sup>.** The dependence of fluorescence emission of TPE-COOH on the concentration of Al<sup>3+</sup> was investigated by incubation with Al<sup>3+</sup> at concentrations ranging from 0.1 to 50 μM. As shown in Figure 2a, the fluorescence at 470 nm enhances gradually as the Al<sup>3+</sup> concentration increases. A linear range for Al<sup>3+</sup> detection can be determined within 0.1–5 μM ( $R^2 = 0.9953$ ) (Figure S-10, Supporting Information). The detection limit of TPE-COOH toward Al<sup>3+</sup> is calculated to be 21.6 nM (signal/noise = 3:1), which was much lower than many previously reported fluorescence probes.<sup>12,16,17,32,34,37</sup> Such high sensitivity is enough to satisfy the U.S. EPA and FDA guidelines of 7.41 μM Al<sup>3+</sup> for bottled drinking water. The feasibility of the probe for the quantitative determination of Al<sup>3+</sup> in aqueous samples was verified by testing bottled drinking water (Supporting Information).

According to Job's Plot analysis (Figure S-11 in the Supporting Information), Al<sup>3+</sup> and TPE-COOH forms a 1:4

complex. To better understanding their binding behavior, <sup>1</sup>H NMR and FT-IR characterization were performed. In <sup>1</sup>H NMR spectra (Figure 2b), as Al<sup>3+</sup> contents increased, the methylene protons shifted downfield from 4.347 to 4.376 ppm, suggesting that the electron deficient Al<sup>3+</sup> probably binds the carboxyl group on TPE-COOH and withdraws electron density from the adjacent methylene. It is also noticeable that with an increased amount of Al<sup>3+</sup>, signals of all TPE-COOH protons diminished. This phenomenon is consistent with the formation of nanoaggregates between TPE-COOH and Al<sup>3+</sup>, which thus reduced the content of free TPE-COOH in solution. In FT-IR spectra (Figure S-12 in the Supporting Information), the band broadening and shifts of –COOH stretching vibrations toward low wavenumber further confirmed the binding effect of Al<sup>3+</sup> on the carboxyl group. On the basis of these results, coordinate bonds were formed between the carboxylic groups of four TPE-COOH molecules and a central Al<sup>3+</sup> (Figure 2b). The resultant spatial structure may just fit the ion size of Al<sup>3+</sup> and thus leads to the selective fluorescence turn-on of the probe.

**Imaging Detection of Al<sup>3+</sup> in Living Cells.** The good stability of the fluorescence switched on by Al<sup>3+</sup> in the pH range of 3.0–7.4 provides the probe with good suitability for the application in bioimaging of living cells (Figure S-13, Supporting Information). As shown in Figure 3a, no background fluorescence was observed from HeLa cells themselves, suggesting that autofluorescence from the cells can be avoided under this condition. For the Al<sup>3+</sup>-loaded HeLa cells, a strong blue fluorescence was detected after incubation with TPE-COOH (Figure 3b), demonstrating the membrane penetra-

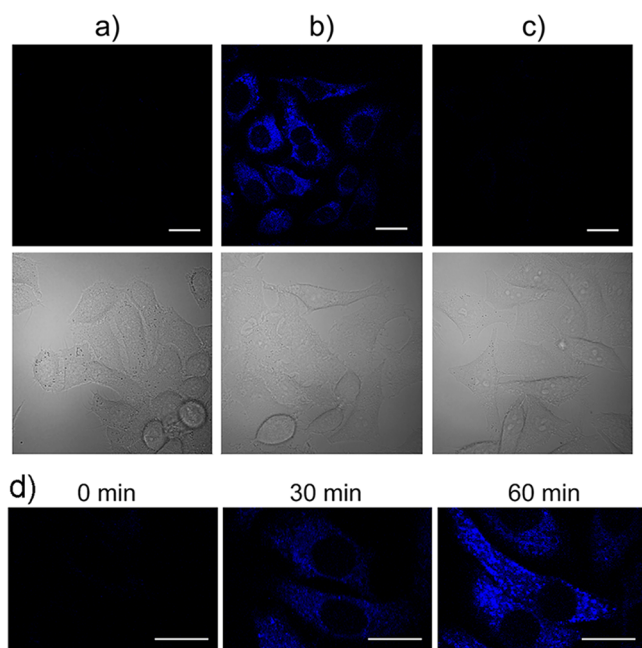


**Figure 3.** CLSM images of HeLa cells (a) without any treatment, (b) after sequentially incubated with  $\text{Al}^{3+}$  ( $50 \mu\text{M}$ ) and TPE-COOH ( $20 \mu\text{M}$  in HEPES containing 2% DMSO), (c) only treated with TPE-COOH ( $20 \mu\text{M}$  in HEPES containing 2% DMSO). Upper panel, blue channel with excitation at 405 nm; lower panel, bright field. (d) Monitoring of the binding process of TPE-COOH to  $\text{Al}^{3+}$ -loaded cells. Scale bar:  $20 \mu\text{m}$ .

bility of TPE-COOH and the complexation with  $\text{Al}^{3+}$  inside the cells. It is noticeable that thanks to the AIE character of TPE-COOH, a very high signal-to-noise imaging of the cell was achieved without any washing steps. Moreover, no fluorescence signal was detected in cells only treated with TPE-COOH (Figure 3c), clearly demonstrating that  $\text{Al}^{3+}$  and its interaction with TPE-COOH are essential for the fluorescence turn-on.

To monitor the binding process of TPE-COOH to intracellular  $\text{Al}^{3+}$ , a time-course assay was performed. Initially, no fluorescence was detected in  $\text{Al}^{3+}$ -loaded cells (Figure 3d). After incubation for 30 min, blue fluorescence signal was observed inside the cells, suggesting the internalization of TPE-COOH and its binding to the preloaded  $\text{Al}^{3+}$  (Figure 3d). As the incubation time was prolonged to 60 min, a greatly intensified fluorescence was identified in the cytoplasm (Figure 3d). With longer incubation, no obvious change in fluorescence intensity was detected, indicating the saturated binding between the probe and  $\text{Al}^{3+}$ . The cytotoxicity of the probe was examined by the standard 3-(4,5-dimethylthiazol-2-yl)-2,5-diphenyltetrazolium bromide (MTT) assay. After incubation with TPE-COOH for 16 h, HeLa cells remained >95% viability (Figure S-14 in the Supporting Information), revealing good biocompatibility of TPE-COOH for bioanalysis.

## CONCLUSION

In this work, a new fluorescence turn-on probe for  $\text{Al}^{3+}$  has been developed based on the AIE effect of tertaphenylethylene and the recognition ability of carboxyl group. The probe exhibits good water solubility and high selectivity and sensitivity for quantitation in an aqueous environment. It is non-fluorescent in solution, while highly emissive upon targetable recognition and complexation of  $\text{Al}^{3+}$  even in very complicated mixtures. Taking advantage of the AIE behavior, its

fluorescence turn-on response to  $\text{Al}^{3+}$  allows the imaging detection and real-time monitoring of  $\text{Al}^{3+}$  in living HeLa cells with a high signal-to-noise ratio.

## ASSOCIATED CONTENT

### Supporting Information

Additional details of a complete description of chemicals, materials, instrumentation, method, characterization, and quantitation determination results. This material is available free of charge via the Internet at <http://pubs.acs.org>.

## AUTHOR INFORMATION

### Corresponding Authors

\*Phone: 86-10-62557910. Fax: 86-10-62559373. E-mail: zhaorui@iccas.ac.cn.

\*E-mail: yanliushui@nchu.edu.cn.

\*E-mail: dqzhang@iccas.ac.cn.

### Notes

The authors declare no competing financial interest.

## ACKNOWLEDGMENTS

This work is supported by grants from the National Natural Science Foundation of China (Grants 21135006, 21375134, 21321003, and 21475140), Ministry of Science and Technology of China (Grant 2015CB856303), and ICCAS (Grant CMS-PY-201308).

## REFERENCES

- (1) Sen, S.; Mukherjee, T.; Chattopadhyay, B.; Moirangthem, A.; Basu, A.; Marek, J.; Chattopadhyay, P. *Analyst* **2012**, *137*, 3975–3981.
- (2) Hornung, V.; Bauernfeind, F.; Halle, A.; Samstad, E. O.; Kono, H.; Rock, K. L.; Fitzgerald, K. A.; Latz, E. *Nat. Immunol.* **2008**, *9*, 847–856.
- (3) Kochian, L. V. *Annu. Rev. Plant. Phys.* **1995**, *46*, 237–260.
- (4) Verstraeten, S.; Aimo, L.; Oteiza, P. *Arch. Toxicol.* **2008**, *82*, 789–802.
- (5) Perl, D. P.; Brody, A. R. *Science* **1980**, *208*, 297–299.
- (6) Cannon, J. R.; Greenamyre, J. T. *Toxicol. Sci.* **2011**, *124*, 225–250.
- (7) Wang, J.; Lin, W.; Li, W. *Chem.—Eur. J.* **2012**, *18*, 13629–13632.
- (8) Zhang, J. Y.; Xing, B. L.; Song, J. Z.; Zhang, F.; Nie, C. Y.; Jiao, L.; Liu, L. B.; Lv, F. T.; Wang, S. *Anal. Chem.* **2014**, *86*, 346–350.
- (9) Feng, L. H.; Zhu, C. L.; Yuan, H. X.; Liu, L. B.; Lv, F. T.; Wang, S. *Chem. Soc. Rev.* **2013**, *42*, 6620–6633.
- (10) Yuan, L.; Lin, W.; Zheng, K.; Zhu, S. *Acc. Chem. Res.* **2013**, *46*, 1462–1473.
- (11) Cao, L.; Jia, C. M.; Huang, Y.; Zhang, Q.; Wang, N.; Xue, Y. L.; Du, D. L. *Tetrahedron Lett.* **2014**, *55*, 4062–4066.
- (12) Fu, Y.; Jiang, X. J.; Zhu, Y. Y.; Zhou, B. J.; Zang, S. Q.; Tang, M. S.; Zhang, H. Y.; Mak, T. C. W. *Dalton Trans.* **2014**, *43*, 12624–12632.
- (13) Kang, R. X.; Shao, X. M.; Peng, F. F.; Zhang, Y. L.; Sun, G. T.; Zhao, W. L.; Jiang, X. D. *RSC Adv.* **2013**, *3*, 21033–21038.
- (14) Peng, L.; Zhou, Z. J.; Wang, X. Y.; Wei, R. R.; Li, K.; Xiang, Y.; Tong, A. J. *Anal. Chim. Acta* **2014**, *829*, 54–59.
- (15) Shellaiah, M.; Wu, Y. H.; Lin, H. C. *Analyst* **2013**, *138*, 2931–2942.
- (16) Barba-Bon, A.; Costero, A. M.; Gil, S.; Parra, M.; Soto, J.; Martinez-Manez, R.; Sancenon, F. *Chem. Commun.* **2012**, *48*, 3000–3002.
- (17) Shi, X.; Wang, H.; Han, T.; Feng, X.; Tong, B.; Shi, J.; Zhi, J.; Dong, Y. *J. Mater. Chem.* **2012**, *22*, 19296–19302.
- (18) Qin, J. C.; Li, T. R.; Wang, B. D.; Yang, Z. Y.; Fan, L. *Spectrochim. Acta, Part A: Mol. Biomol. Spectrosc.* **2014**, *133*, 38–43.
- (19) Ding, D.; Li, K.; Liu, B.; Tang, B. Z. *Acc. Chem. Res.* **2013**, *46*, 2441–2453.

- (20) Shustova, N. B.; McCarthy, B. D.; Dinca, M. J. *Am. Chem. Soc.* **2011**, *133*, 20126–20129.
- (21) Hong, Y. N.; Lam, J. W. Y.; Tang, B. Z. *Chem. Soc. Rev.* **2011**, *40*, 5361–5388.
- (22) Wang, M.; Zhang, G. X.; Zhang, D. Q.; Zhu, D. B.; Tang, B. Z. *J. Mater. Chem.* **2010**, *20*, 1858–1867.
- (23) Zhang, G. X.; Hu, F.; Zhang, D. Q. *Langmuir* **2014**, DOI: 10.1021/la5029367.
- (24) Huang, G. X.; Zhang, D. Q. *Chem. Commun.* **2012**, *48*, 7504–7506.
- (25) Bian, N.; Chen, Q.; Qiu, X. L.; Qi, A. D.; Han, B. H. *New J. Chem.* **2011**, *35*, 1667–1671.
- (26) Wang, M.; Zhang, D. Q.; Zhang, G. X.; Tang, Y. L.; Wang, S.; Zhu, D. B. *Anal. Chem.* **2008**, *80*, 6443–6448.
- (27) Shi, H. B.; Liu, J. Z.; Geng, J. L.; Tang, B. Z.; Liu, B. J. *Am. Chem. Soc.* **2012**, *134*, 9569–9572.
- (28) Hu, F.; Huang, Y. Y.; Zhang, G. X.; Zhao, R.; Yang, H.; Zhang, D. Q. *Anal. Chem.* **2014**, *86*, 7987–7995.
- (29) Huang, Y. Y.; Hu, F.; Zhao, R.; Zhang, G. X.; Yang, H.; Zhang, D. Q. *Chem.—Eur. J.* **2014**, *20*, 158–164.
- (30) Han, T. Y.; Feng, X.; Tong, B.; Shi, J. B.; Chen, L.; Zhi, J. G.; Dong, Y. P. *Chem. Commun.* **2012**, *48*, 416–418.
- (31) Chen, X. J.; Shen, X. Y.; Guan, E. J.; Liu, Y.; Qin, A. J.; Sun, J. Z.; Tang, B. Z. *Chem. Commun.* **2013**, *49*, 1503–1505.
- (32) Wei, T.-T.; Zhang, J.; Mao, G.-J.; Zhang, X.-B.; Ran, Z.-J.; Tan, W.; Yu, R. *Anal. Methods* **2013**, *5*, 3909–3914.
- (33) Du, X.; Qu, J.; Zhang, Z.; Ma, D.; Wang, Z. *Chem. Mater.* **2012**, *24*, 2178–2185.
- (34) Jia, T. J.; Cao, W.; Zheng, X. J.; Jin, L. P. *Tetrahedron Lett.* **2013**, *54*, 3471–3474.
- (35) Xu, K. J.; Hong, M. W.; Zhang, Y. C.; Song, L.; Chai, W. X. *Acta Crystallogr.* **2014**, *70*, 858–861.
- (36) Sankaralingam, M.; Balamurugan, M.; Palaniandavar, M.; Vadivelu, P.; Suresh, C. H. *Chem.—Eur. J.* **2014**, *20*, 11346–11361.
- (37) Samanta, S.; Goswami, S.; Hoque, Md. N.; Ramesh, A.; Das, G. *Chem. Commun.* **2014**, *50*, 11833–11836.